Received: 30 March 2021 | Revised: 22 July 2021 | Accepted: 6 October 2021

DOI: 10.1111/ejss.13182

ORIGINAL ARTICLE

European Journal of Soil Science WILEY

Slope threshold for overland flow resistance on sandy soils

Alessio Nicosia | Gaetano Guida | Costanza Di Stefano | Vincenzo Pampalone | Vito Ferro

Department of Agricultural, Food and Forest Sciences, University of Palermo, Palermo, Italy

Correspondence
Vito Ferro, Department of Agricultural, Food and Forest Sciences, University of Palermo, Palermo.
Email: vito.ferro@unipa.it

Funding information
Open Access Funding provided by Universita degli Studi di Palermo within the CRUI-CARE Agreement.

Abstract

Recent research on rill flows recognised that an 18% slope can be used to distinguish between 'gentle' and 'steep' slope cases for the detected differences in hydraulic (flow depth and velocity) and sediment transport variables (flow transport capacity, actual sediment load). The effects of slope on flow velocity, friction factor and transport capacity and their interactions affect process-based erosion modelling. The main aim of this paper is to investigate, for the first time, how slope affects the overland flow resistance on sandy soils, which are characterised by loose particles readily available to be transported and deposited. Using literature measurements carried out in sandy soils for both gentle and steep slopes, a theoretical overland flow resistance equation, based on the integration of the power velocity distribution, is tested. The relationship between the velocity profile parameter Γ, the channel slope, the Reynolds and Froude number is calibrated using measurements characterized by a wide range of hydraulic conditions and distinguishing between gentle (5.2%–13.2%) and steep (17.4%–42.3%) slope conditions. The analysis demonstrated that: (1) the parameter Γ can be accurately estimated by Equation (15) in which the exponents are independent of slope condition; (2) the coefficient a of Equation (15) is equal to 0.8750 and 0.8984 for the gentle and steep slope condition, respectively; (3) the estimations of the Darcy–Weisbach friction factor f (Equation 19) are accurate and characterised by errors less than or equal to ±5% for 97.2% of cases; and (4) in the range of steep slopes, the flow resistance law calibrated for the gentle slope condition (Equation (19) with $a = 0.8750$) systematically overestimates the f value. In conclusion, this study allowed the recognition, for an unlimited soil detachment condition and an overland flow, of how the energy dissipation processes and the estimate of the friction factor are affected by slope.

Highlights

- A theoretical overland flow resistance law is tested by data obtained on sandy soils.

This is an open access article under the terms of the Creative Commons Attribution License, which permits use, distribution and reproduction in any medium, provided the original work is properly cited.
© 2021 The Authors. *European Journal of Soil Science* published by John Wiley & Sons Ltd on behalf of British Society of Soil Science.

- Differences between gentle and steep slope conditions are investigated.
- The Darcy–Weisbach friction factor estimate by the flow resistance law is accurate.
- The law calibrated for gentle slopes overestimates f in the range of steep slopes.

KEYWORDS

flow resistance, gentle hillslopes, overland flow hydraulics, soil erosion, steep hillslopes

1 | INTRODUCTION

Among various land degradation processes, soil erosion is considered as a relevant environmental problem causing loss of topsoil and nutrients, reducing soil fertility and, as a consequence, crop production (Di Stefano & Ferro, 2016). Moreover, soil erosion is considered a geomorphological and a geological hazard as it may give a rise to property and infrastructure damage, loss of livelihoods and services, and environmental damage (Poesen, 2018).

Process-oriented models generally distinguish the soil erosion process into interrill and rill erosion (Toy et al., 2002). The main reason to apply this interrill-rill scheme is that a different behaviour, with respect to the variables controlling the physical process, distinguishes interrill from rill erosion. Interrill areas are characterised by soil detachment mainly due to raindrops' impact and sediment transport by overland flow from these areas to rill channels. In particular, soil detachment action is due to rainsplash while sediment transport is due to a thin flow, characterised by low bottom shear stresses, which has a negligible detachment capacity. According to this physical scheme (Nearing et al., 1989), raindrop impact causes soil particle detachment while overland flow is simply able to transport the detached particles to rill areas.

In this context, the evaluation of overland flow velocity is required to estimate flow transport capacity T_c and is strictly related to the knowledge of flow resistance. Slope appreciably affects T_c, defined as the maximum equilibrium sediment load that a flow can transport (Abrahams et al., 2001; Ali et al., 2011, 2012; Ferro, 1998), and, for this reason, is a hydraulic variable limiting soil detachment rate and actual sediment transport.

According to previous research (Everaert, 1991; Govers, 1990; Zhang et al., 2009), the effect of slope on flow transport capacity should vary from erodible to non-erodible bed conditions as the roughness of erodible beds is always higher than that of non-erodible beds. Govers (1990) and Everaert (1991) stated that for erodible beds the effect of slope on transport capacity is higher than that due to unit discharge. The experimental runs by Zhang et al. (2009), carried out using a non-erodible bed, established the opposite result: that transport capacity is more sensitive to unit discharge as compared to slope.

Sajjadi and Mahmoodabadi (2015) investigated a rain-induced overland flow using a tray, having a slope gradient ranging from 0.5% to 20% (gentle slope condition), two rainfall intensities (57 and 80 mm h^{-1}) and two soils having a sand content of 56.6%–58.8%. This study demonstrated that sediment concentration increases with slope gradient and that overland flow velocity is the best predictor of sediment concentration among the studied hydraulic variables (flow depth, shear stress, stream power and unit stream power). The investigation does not allow the recognition of the effect of steep slopes on the hydraulic and sedimentological variables and to assess if a slope threshold can be established for an overland flow.

Xiao et al. (2017a) studied the combined effects of slope gradient, varying in the range 17.6%–46.6%, and hydraulic variables on soil detachment rate and sediment transport capacity of rill flows. The measurements, carried out on a slope-adjustable plot with a loessial soil (clay 9.08%, silt 59.59% and sand 31.33%), indicated that soil detachment rate varies linearly with discharge and exponentially with slope. The same trends with discharge and slope were detected for the sediment transport capacity (Xiao et al., 2017b).

No slope threshold can be established for the channelised rill flows investigated by Xiao et al. (2017a, 2017b) as all measurements were performed on steep slopes.

Jiang et al. (2018) stated that the hydraulic mechanisms of soil erosion for steep slopes are different from those acting on gentle slopes. Testing of available T_c equations using slopes steeper than 18% (Ali et al., 2013; Wu et al., 2016; Zhang et al., 2009) allowed the conclusion that T_c relationships developed for 'gentle' slopes (<18%) are unsuitable to be applied to 'steep' slopes (17%–47%). Also, Peng et al. (2015) noticed that 'there has been little research concerning rill flow on steep slopes (e.g., slope gradients higher than 10°)' and highlighted that the

relationship between the roughness coefficient and the Reynolds number is greatly dependent on the slope gradient. For slope values greater than or equal to 18%, the measurements by Peng et al. (2015) were characterised by supercritical flows ($1.08 \leq F \leq 2.33$, where $F = V/(gh)^{0.5}$ is the Froude number of the flow, V is the mean flow velocity, g is acceleration due to gravity and h is water depth) with a flow regime varying from transitional to turbulent ($1240 \leq Re \leq 7629$, where $Re = Vh/\nu_k$ is the Reynolds number and ν_k is the water kinematic viscosity). According to these results, for taking into account differences in hydraulic (flow depth, velocity, Reynolds number, Froude number) and variables related to sediment transport (flow transport capacity, actual sediment load), the slope of 18% can be considered to distinguish between the gentle slope and the steep slope case.

Di Stefano et al. (2021) used data on mobile bed rill channels joined with measurements carried out in rill flumes, in which the sediment load of the flow was equal to its transport capacity, to test the applicability of a theoretical rill flow resistance law. Using a database constituted by measurements characterised by high slope values (17.6%–84%) and a wide range of textural fractions, Di Stefano et al. (2021) demonstrated that Darcy–Weisbach friction factor is affected by the soil particle detachability and transportability of the investigated soil.

Therefore, previous studies demonstrated that a slope threshold of 18% can be used to distinguish two different slope conditions (gentle and steep) for rill flows. Rill erosion is due to the detachment and transport of soil particles and aggregates by concentrated flows while overland flow has to be considered as a 'disturbed laminar flow' because the impact of raindrops causes both an increase of flow turbulence and a retarding effect on flow velocity (Emmett, 1970). Therefore, the applicability of the slope threshold of 18%, originally deduced for rill flows, has to be proved for overland flows.

A limitation in simulating overland flow by hillslope-scale runoff models is that the use of hydraulic equations, such as Manning and Darcy–Weisbach, is extremely simplistic (Smith et al., 2007), and the resistance coefficient changes for different surface conditions (Kowobari et al., 1972). The shaping action of hillslope, due to the interaction among the flow characteristics, sediment transport and the erodible wetted perimeter, limits the applicability of the uniform flow equations developed for large and fixed beds. However, the frequent unavailability of measured velocity distributions in different verticals of a cross-section and the complexity of the integration procedure justify the use of these empirical flow resistance equations expressed as (Ferro, 1999; Powell, 2014):

$$V = \frac{s^{1/2}\, R^{2/3}}{n} = \sqrt{\frac{8gRs}{f}}, \quad (1)$$

in which V (m s^{-1}) is the cross-section average velocity, n (m$^{-1/3}$ s) is Manning coefficient, f is Darcy–Weisbach friction factor, s is slope gradient, R (m) is hydraulic radius and g (m s^{-2}) is acceleration due to gravity. Field and laboratory studies on overland flows generally use the Darcy–Weisbach friction factor, while the use of Manning's n is widespread in open channel flows (Hessel et al., 2003). However, this differentiation is not well-defined and 'Manning's n is likely to behave in the same way as f' (Hessel et al., 2003; Takken & Govers, 2000). The Darcy–Weisbach friction factor is currently applied in Water Erosion Prediction Project model (Foster et al., 1995; Govers et al., 2007; Nicosia et al., 2019).

Recently, Nicosia et al. (2020a, 2020b, 2020c) extended the applicability of a theoretical resistance law deduced for open channel flow (Ferro, 2017, 2018a, 2018b; Ferro & Porto, 2018a, 2018b) to the overland flow case. This theoretical flow resistance equation, based on the integration of a power velocity distribution, was tested using literature databases obtained for different roughness conditions. In particular, the data-bases by Yoon and Wenzel (1971), Nearing et al. (2017) and Polyakov et al. (2018), obtained by experiments carried out on a smooth bed, a rough bed and a rough bed with vegetation cover were used, respectively.

Sandy soils are characterised by loose particles readily available to be transported and deposited and their use allows the investigation of unlimited detachment conditions. Taking into account that for a sandy soil the control of the flow detachment capability is not required, the experimental investigation can be carried out by a flume in which the overland flow is not subjected to the effect of rainfall impact.

In this paper, the flow hydraulic variables (water depth h, slope gradient s, mean velocity V, Reynolds number Re, Froude number F, and Darcy–Weisbach friction factor f) measured in laboratory flume by Ali et al. (2012) and Zhang et al. (2011) were used to test the applicability of the theoretical overland flow resistance equation. The latter has been modified from Nicosia, Di Stefano, Palmeri, Pampalone, and Ferro (2020a); Nicosia, Di Stefano, Pampalone, Palmeri, Ferro, and Nearing (2020b); and Nicosia, Di Stefano, Pampalone, Palmeri, Ferro, Polyakov, and Nearing (2020c) for considering the effect of the flow Reynolds number and was also specifically calibrated for sandy soils distinguishing the gentle from the steep slope condition. To the best of our knowledge, the database used in this investigation (96 measurements) consists of all available measurements for overland flows on sandy soils

and it is representative of a wide range of slope gradient ($5.2\% \le s \le 42.3\%$), flow regimes ($55 \le Re \le 3302$) and hydraulic conditions ranging from subcritical to supercritical ($0.54 \le F \le 6.78$).

2 | THE OVERLAND FLOW RESISTANCE EQUATION

The use of dimensional analysis and self-similarity theory (Barenblatt, 1979, 1987) allows the theoretical deduction of the flow velocity distribution in an open channel flow (Ferro, 2017, 2018a, 2018b). For an overland flow on a hillslope, the local flow velocity distribution $v(y)$ along a given vertical is expressed by the following functional equation (Barenblatt, 1987, 1993; Ferro, 1997):

$$\phi\left(\frac{dv}{dy}, y, h, d, u_*, s, \rho, \mu, g\right) = 0, \tag{2}$$

in which ϕ is a functional symbol, y is the distance from the bottom, d is a characteristic diameter of the soil particles, $u_* = \sqrt{g R s}$ is the shear velocity, ρ is the water density, and μ is the water viscosity.

Applying the Π-theorem (Barenblatt, 1987), Equation (2) can be rewritten in the following dimensionless form:

$$\Pi_1 = \phi_2(\Pi_2, \Pi_3, \Pi_4, \Pi_5, \Pi_6), \tag{3}$$

in which Π_1, Π_2, Π_3, Π_4, Π_5 and Π_6 are dimensionless groups and ϕ_2 is a functional symbol.

Using dimensional independent variables y, u_* and μ, to deduce the dimensionless groups, Equation (3) can be rewritten as follows (Ferro, 2018b; Nicosia, Di Stefano, Palmeri, Pampalone, & Ferro, 2020a):

$$\frac{y}{u_*}\frac{dv}{dy} = \phi_2\left(\frac{h}{y}, \frac{d}{y}, s, \frac{u_* y}{\nu_k}, \frac{g y}{u_*^2}\right). \tag{4}$$

Considering that according to Barenblatt (1987) 'In some cases, it turns out to be convenient to choose new similarity parameters—products of powers of the similarity parameters obtained in the previous step', the following dimensionless groups are deduced:

$$\Pi_{2,3} = \frac{\Pi_2}{\Pi_3} = \frac{h}{y}\frac{y}{d} = \frac{h}{d}, \tag{5}$$

$$\Pi_{2,5} = \Pi_2 \Pi_5 = \frac{h}{y}\frac{u_* y}{\nu_k} = \frac{u_* h}{\nu_k} = Re_*, \tag{6}$$

in which Re_* is the shear Reynolds number, and

$$\Pi_{6,2} = \sqrt{\frac{8}{f}}\frac{1}{\Pi_6^{1/2}\Pi_2^{1/2}} = \sqrt{\frac{8}{f}}\frac{u_*}{g^{1/2}y^{1/2}}\frac{y^{1/2}}{h^{1/2}} = \frac{\sqrt{\frac{8u_*^2}{f}}}{g^{1/2}h^{1/2}} = \frac{V}{\sqrt{g h}} = F. \tag{7}$$

Since Ferro (2018b) demonstrated that F takes also into account both the depth sediment ratio h/d and the shear Reynolds number Re_* and considering that Equation (6) can be rewritten as follows:

$$\Pi_{2,5} = \sqrt{\frac{8}{f}}\Pi_2 \Pi_5 = \frac{V}{u_*}\frac{h}{y}\frac{u_* y}{\nu_k} = \frac{V h}{\nu_k} = Re, \tag{8}$$

the functional relationship (Equation 4) becomes:

$$\frac{y}{u_*}\frac{dv}{dy} = \phi_3\left(Re, s, F, \frac{u_* y}{\nu_k}\right), \tag{9}$$

where ϕ_3 is a functional symbol.

Assuming the incomplete self-similarity (ISS) hypothesis in $u_* y/\nu_k$ (Barenblatt & Monin, 1979; Barenblatt & Prostokishin, 1993; Ferro, 2017), Equation (9) can be integrated (Barenblatt & Prostokishin, 1993; Ferro & Pecoraro, 2000) and the following power velocity profile is obtained:

$$\frac{v}{u_*} = \left[\frac{1}{\delta}\phi_4(Re, s, F)\right]\left(\frac{u_* y}{\upsilon_k}\right)^{\delta}, \tag{10}$$

in which ϕ_4 is a functional symbol and δ is an exponent which is calculated by the following theoretical equation (Barenblatt, 1991; Castaing et al., 1990):

$$\delta = \frac{1.5}{\ln Re}. \tag{11}$$

In conclusion, Equation (10) can be rewritten as follows:

$$\frac{v}{u_*} = \Gamma(Re, s, F)\left(\frac{u_* y}{\upsilon_k}\right)^{\delta}, \tag{12}$$

in which Γ is a function of the dimensionless groups Re, s and F to be defined by velocity measurements.

Setting $y = \alpha h$ as the distance from the bottom at which the local velocity is equal to the cross-section average velocity V, Equation (12) gives the following value Γ_v of the Γ function (Ferro, 2017; Ferro & Porto, 2018a):

$$\Gamma_v = \frac{V}{u_* \left(\frac{u_* \alpha h}{\nu_k}\right)^{\delta}}, \quad (13)$$

in which α is a coefficient, smaller than unit, which takes into account that the average velocity V is located under the water surface and that the mean velocity profile, whose integration gives V, is calculated by averaging, for each distance y, the velocity values v measured in different verticals. Ferro (2017) theoretically deduced the following equation for calculating α:

$$\alpha = \left[\frac{2^{1-\delta}}{(\delta+1)(\delta+2)}\right]^{1/\delta}. \quad (14)$$

Applying the ISS for all the dimensionless groups included in the Γ functional relationship (see Equation 12), the following estimate Γ_v is obtained (Ferro, 2018b):

$$\Gamma_v = a \frac{F^b}{s^c\, Re^e}, \quad (15)$$

in which the coefficients *a, b, c* and *e* have to be experimentally determined.

The Darcy–Weisbach friction factor f is obtained by integrating the power velocity distribution (Equation 12) (Barenblatt, 1993; Di Stefano et al., 2017; Ferro, 2017; Ferro & Porto, 2018a, 2018b):

$$f = 8\left[\frac{(\delta+1)(\delta+2)}{2^{1-\delta}\,\Gamma\, 4.4817}\right]^{\frac{2}{1+\delta}} \quad (16)$$

The application of Equation (16) requires the estimations of δ by Equation (11) and $\Gamma = \Gamma_v$ by the calibrated Equation (15).

3 | AVAILABLE LITERATURE DATA

3.1 | Experiments by Ali et al. (2012)

Ali et al. (2012) carried out an experimental investigation using a flume, 0.5 m wide and 6 m long, with an erodible bed and plexiglass banks. Four well sorted non-cohesive medium to very coarse sands (with a median diameter D_{50} equal to 0.233, 0.536, 0.719 and 1.022 mm) constituted the erodible bed over which the flow had a sediment load equal to the transport capacity. For the experiments, the flume bed was adjusted to four slope gradients (5.2%, 8.7%, 13.2% and 17.6%). A calibrated flow-meter at the inlet pipe was used for continuous monitoring of the inflow discharge which ranged from 0.035 to 1.035 L s^{-1}. Two point gauges with an accuracy of 0.1 mm were used to measure the water depth. The data-base is constituted by 63 experimental runs for the gentle slope condition and 18 for the steep one. The 81 experimental runs were carried out for Reynolds numbers of $55 \leq Re \leq 1624$ and Froude numbers ranging from 0.54 to 2.49.

3.2 | Experiments by Zhang et al. (2011)

The flume was 5 m long, 0.4 m wide with smooth glass walls and a plexiglass bed. A 5-mm layer of sieved sediment (<2 mm) was glued on the flume bed to simulate grain roughness. The experimental runs were carried out using a flow transporting a sand (with D_{50} of 0.10, 0.22, 0.41, 0.69 and 1.16 mm) and ensuring that the sediment transport capacity was reached for each combination of flow discharge and slope gradient. For the experiments, the flume bed was adjusted to five slope gradients (8.7%, 17.4%, 25.9%, 34.2% and 42.3%). The flow discharge ranged from 0.264 to 2.104 L s^{-1}. Flow depth was measured with a digital level probe at the section 0.6 m upstream from the outlet. The data-base is constituted by 5 experimental runs for the gentle slope condition and 20 for the steep one. The 25 experimental runs were carried out for Reynolds numbers of $414 \leq Re \leq 3302$ and Froude numbers ranging from 2.18 to 6.78.

4 | RESULTS

The available data-base is characterised by hydraulic regimes ranging from laminar to turbulent ($55 \leq Re \leq 3302$) (Figure 1), flows ranging from subcritical to supercritical ($0.54 \leq F \leq 6.78$), and a wide range of slope gradients ($5.2\% \leq s \leq 42.3\%$) (Figure 2). Figure 1 also shows that, for given *Re*, flows over steep slopes are characterised by higher Froude numbers compared to flows moving on gentle slopes.

Equation (15) for estimating the Γ_v function was calibrated both on the measurements available for the gentle (Equation 17) and steep slope condition (Equation 18) obtaining

$$\Gamma_v = 0.971 \frac{F^{1.262}}{s^{0.6388}\, Re^{0.1618}}, \quad (17)$$

which is characterised by a coefficient of determination R^2 equal to 0.997, and

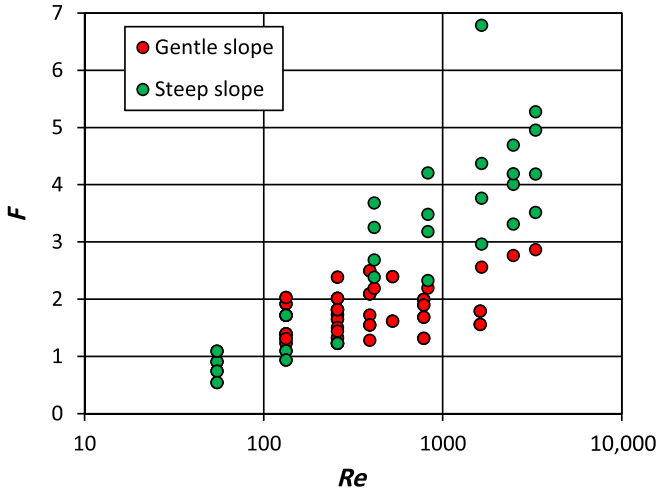

FIGURE 1 Plot of the (Re, F) pairs for the gentle and steep slope condition

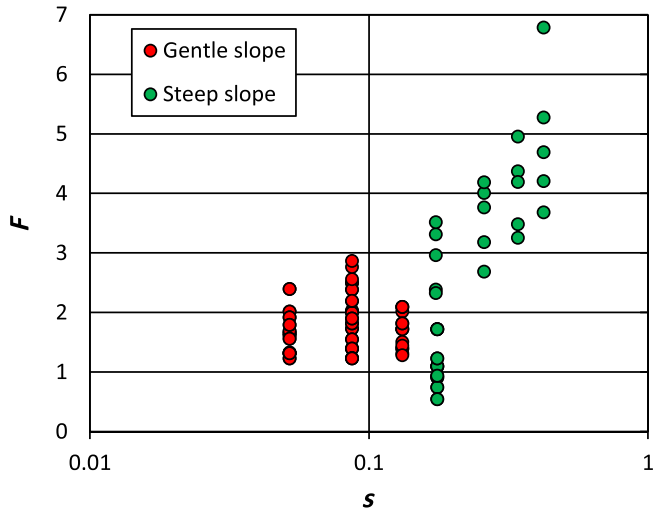

FIGURE 2 Plot of the (s, F) pairs for the gentle and steep slope condition

$$\Gamma_v = 0.924\,\frac{F^{1.274}}{s^{0.6532}\,Re^{0.1552}}, \tag{18}$$

with $R^2 = 0.99$.

For the gentle slope, the comparison between the 68 measured Γ_v values, obtained by Equations (13), (11) and (14), and those calculated by Equation (17) is plotted in Figure 3a, while for the steep slope the comparison between the 38 measured Γ_v values and those calculated by Equation (18) is shown in Figure 3b.

Taking into account that for the two investigated slope conditions the obtained values of the exponents b, c and e of Equations (17) and (18) are similar, the measured Γ_v values were plotted against to those of the

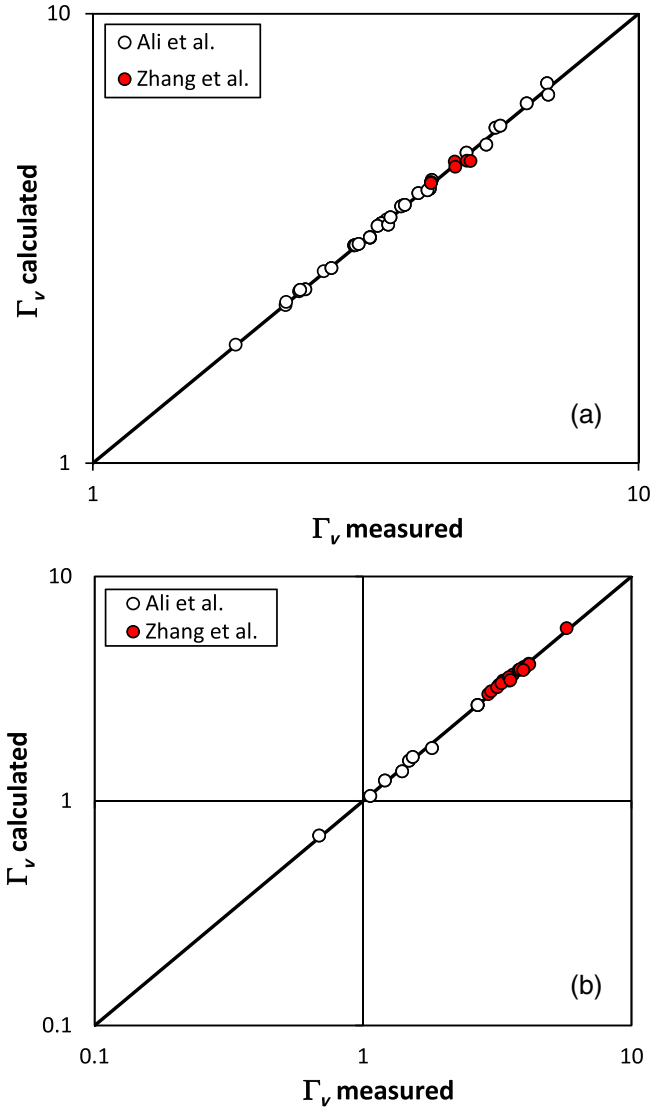

FIGURE 3 Comparison between the measured Γ_v values, obtained by Equations (13), (11) and (14), and those calculated by (a) Equation (17) and (b) Equation (18)

variable $x = F^{1.27}\,s^{-0.65}\,Re^{-0.15}$. Figure 4 shows the relationship between Γ_v and x which allows the estimation of $a = 0.8750$ for the gentle slope (Figure 4a) and $a = 0.8984$ for the steep slope (Figure 4b). Substituting Equation (15) with $b = 1.27$, $c = 0.65$ and $e = 0.15$ into Equation (16), the following flow resistance law is obtained:

$$f = 8\left[\frac{(\delta+1)\,(\delta+2)}{4.4817\;2^{1-\delta}\,a}\,\frac{Re^{0.15}\,s^{0.65}}{F^{1.27}}\right]^{\frac{2}{1+\delta}}. \tag{19}$$

The good agreement between the measured f values of the considered data base and those calculated by Equation (19) is shown in Figure 5.

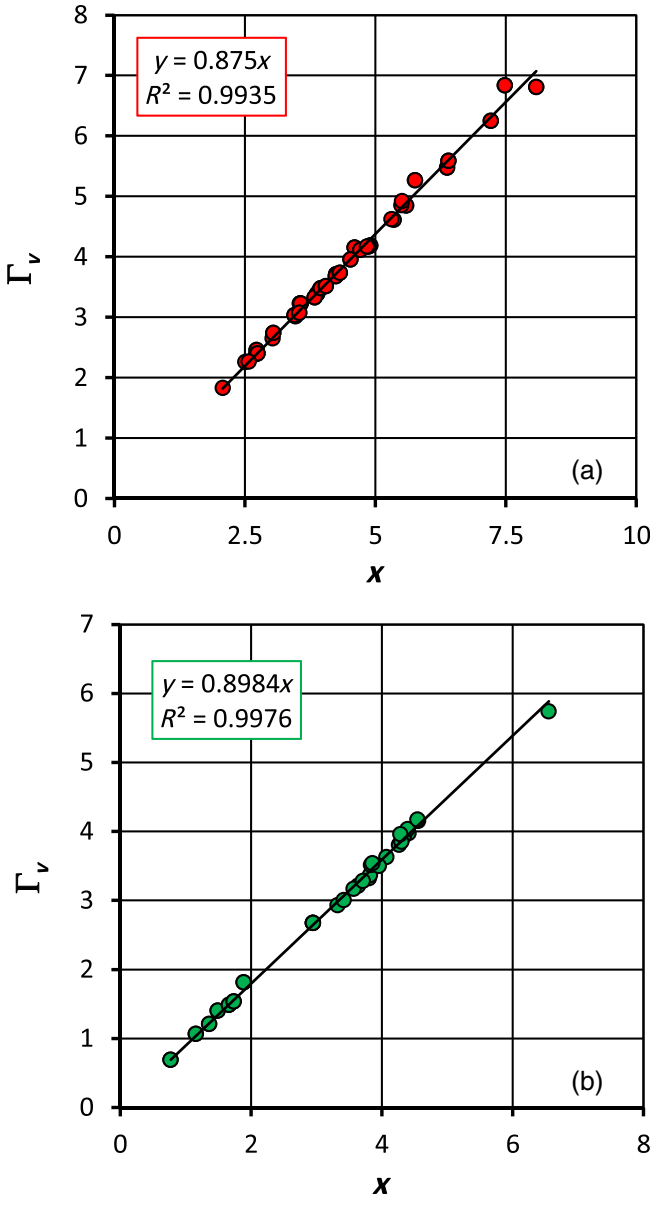

FIGURE 4 Relationship between the measured Γ_v values, obtained by Equations (13), (11) and (14), and the variable x for (a) the gentle and (b) steep slope condition

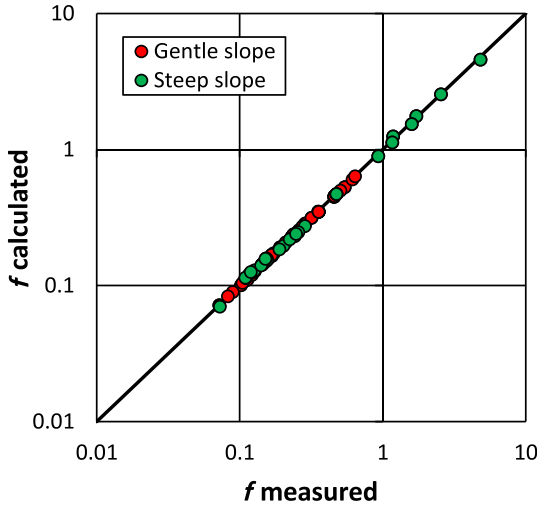

FIGURE 5 Comparison between the measured Darcy–Weisbach friction factor values and those calculated by the theoretical flow resistance equation (Equation 19)

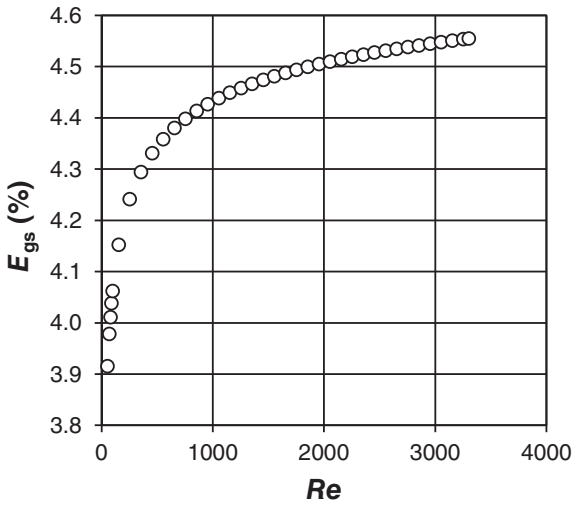

FIGURE 6 Estimate errors of the Darcy–Weisbach friction factor obtained applying Equation (19) calibrated for gentle slopes to steep slopes

The latter are characterised by errors $E = 100\,(f_{calculated} - f_{measured})/f_{measured}$ lower than or equal to ±5% for 97.2% of cases and lower than or equal to ±3% for 79.2% of cases.

The ratio between the calculated Darcy–Weisbach friction factor for the steep slope, named f_{steep} (Equation (19) with $a = 0.8984$), and that calculated for the gentle slope, named f_{gentle} (Equation (19) with $a = 0.8750$), follows as:

$$\frac{f_{steep}}{f_{gentle}} = \left(\frac{0.8984}{0.8750}\right)^{-\frac{2}{1+\delta}} = 1.027^{-\frac{2}{1+\delta}}, \qquad (20)$$

and is always less than 1. In other words, for given values of Re, F and s, the calculated value f_{gentle} is always greater than the calculated value f_{steep}. Applying f_{gentle} to estimate the Darcy–Weisbach friction factor for a steep slope condition, the error $E_{gs} = 100\,(f_{gentle} - f_{steep})/f_{steep}$ is expressed as:

$$E_{gs} = 100\left(\frac{f_{gentle}}{f_{steep}} - 1\right) = 100\left(1.027^{\frac{2}{1+\delta}} - 1\right), \qquad (21)$$

and, in the range of the investigated Re values, varies from 3.9% to 4.5% (Figure 6).

5 | DISCUSSION

For a sandy soil, Figure 3 shows a good agreement between the calibration data and Equation (17) or (18). The actual sediment transport is the result of the interaction between the flow characteristics, which are represented by the sediment transport capacity T_c (Ferro, 1998), and soil particle properties. These are described by their aptitude to be detached from the wetted perimeter (detachability) and to be transported (transportability), which is related to particle size and specific weight. All sandy soil data used to calibrate Equation (15) are characterised by comparable soil properties (i.e., high detachability and low transportability) and, therefore, the effect of sediment transport on overland flow resistance depends only on sediment transport capacity. Many studies demonstrated that sediment transport capacity increases as a power function of slope gradient (Prosser & Rustomji, 2000; Xiao et al., 2017a; Zhang et al., 2011) which, consequently, surrogates the effect of sediment transport on flow resistance. Finally, the component of flow resistance due to sediment transport is greater in steep than in gentle slopes. This implies that, in the absence of bed-forms and for given grain roughness, the friction factor increases in the passage from gentle to steep slopes.

The f relationship derived for gentle slopes is not applicable to data obtained for steep slopes as, although errors are close to those obtained with the f relationship derived for steep slopes, it gives biased predictions of the friction factor. This systematic error can be physically justified considering that f_{gentle} is applied to equilibrium sediment transport condition in which the actual sediment load is that of the steep condition while the transport capacity corresponds to the gentle slope. In other words, f_{gentle} is calculated assuming an overestimated sediment load, that is, greater than the flow transport capacity for gentle slopes.

In conclusion, the distinction between gentle and steep slopes allows the proper consideration of the effect of sediment transport on the estimate of the friction factor for overland flow on sandy soils.

6 | CONCLUSIONS

The applicability of classical hydraulic formulations, such as Chezy or Manning's equations, for mobile bed overland flow can be limited by the need to consider the effects of the interaction between flow, bed morphology and sediment transport.

The available data on mobile bed overland flows, in which the sediment load was equal to the transport capacity, were used to test the applicability of a theoretical flow resistance law. This data-base was constituted by measurements performed on sandy soils for gentle (5.2%–8.7%) and steep (17.4%–42.3%) slope conditions.

The analysis demonstrated that the velocity profile parameter Γ can be accurately estimated by Equation (15), in which only the coefficient a depends on the slope condition. Also, the estimations of the Darcy–Weisbach friction factor by the theoretical flow resistance law (Equation 19) are accurate inasmuch as they are characterised by errors that are almost always less than $\pm 5\%$. In the range of steep slopes, the flow resistance calibrated for the gentle slope condition (Equation (19) with $a = 0.8750$) gives a systematic overestimation of the friction factor.

Finally, the distinction between gentle and steep slope conditions allowed accounting for a different sediment transport effect on overland flow resistance.

ACKNOWLEDGEMENT

Open access funding enabled and organized by Projekt DEAL.

CONFLICT OF INTEREST

The authors have no conflict of interest to declare.

DATA AVAILABILITY STATEMENT

Data are published on the papers by Ali et al. (2012) and Zhang et al. (2011).

AUTHOR CONTRIBUTIONS

Alessio Nicosia: Conceptualization (equal); methodology (equal); validation (equal); writing – original draft (equal); writing – review and editing (equal). **Gaetano Guida:** Conceptualization (equal); methodology (equal); validation (equal); writing – original draft (equal); writing – review and editing (equal). **Costanza Di Stefano:** Conceptualization (equal); methodology (equal); validation (equal); writing – original draft (equal); writing – review and editing (equal). **Vincenzo Pampalone:** Conceptualization (equal); methodology (equal); validation (equal); writing – original draft (equal); writing – review and editing (equal). **V Ferro:** Conceptualization (equal); methodology (equal); validation (equal); writing – original draft (equal); writing – review and editing (equal).

ORCID

Gaetano Guida https://orcid.org/0000-0002-7718-4392
Vito Ferro https://orcid.org/0000-0003-3020-3119

REFERENCES

Abrahams, A. D., Li, G., Krishana, C., & Atkinson, J. F. (2001). A sediment transport equation for interrill overland flow on rough

surface. *Earth Surface Processes and Landforms*, *26*(1443–1459), 2001.

Ali, M., Seeger, M., Sterk, G., & Moore, D. (2013). A unit stream power based sediment transport function for overland flow. *Catena*, *101*, 197–204.

Ali, M., Sterk, G., Seeger, M., Boersema, M., & Peters, P. (2012). Effect of hydraulic parameters on sediment transport capacity in overland flow over erodible beds. *Hydrology and Earth System Sciences*, *16*, 591–601. https://doi.org/10.5194/hess-16-591-2012

Ali, M., Sterk, G., Seeger, M., & Stroosnijder, L. (2011). Effect of hydraulic parameters on sediment transport capacity in overland flow over erodible beds. *Hydrology and Earth System Sciences Discussions*, *8*(4), 6939–6965.

Barenblatt, G. I. (1979). *Similarity, self-similarity and intermediate asymptotics*. Consultants Bureau, New York.

Barenblatt, G. I. (1987). *Dimensional analysis*. Gordon & Breach, Science Publishers.

Barenblatt, G. I. (1991). On the scaling laws (incomplete self-similarity with respect to Reynolds numbers) for the developed turbulent flows in tubes. *Comptes Rendus de l'Académie des Sciences - Series IIA*, *313*, 307–312.

Barenblatt, G. I. (1993). Scaling laws for fully developed turbulent shear flows, part 1, basic hypothesis and analysis. *Journal of Fluid Mechanics*, *248*, 513–520.

Barenblatt, G. I., & Monin, A. S. (1979). Similarity laws for turbulent stratified flows. *Archive for Rational Mechanics and Analysis*, *70*, 307–317.

Barenblatt, G. I., & Prostokishin, V. M. (1993). Scaling laws for fully developed turbulent shear flows, part 2. Processing of experimental data. *Journal of Fluid Mechanics*, *248*, 521–529.

Castaing, B., Gagne, Y., & Hopfinger, E. J. (1990). Velocity probability density functions of high Reynolds number turbulence. *Phisica D*, *46*, 177–200.

Di Stefano, C., & Ferro, V. (2016). Establishing soil loss tolerance: An overview. *Journal of Agricultural Engineering Research*, *XLVII*, 127–133. https://doi.org/10.4081/jae.2016.560

Di Stefano, C., Ferro, V., Palmeri, V., & Pampalone, V. (2017). Flow resistance equation for rills. *Hydrological Processes*, *31*, 2793–2801.

Di Stefano, C., Nicosia, A., Palmeri, V., Pampalone, V., & Ferro, V. (2021). Estimating flow resistance in steep slope rills. *Hydrological Processes*, *35*(7), e14296.

Emmett, W.W., 1970. *The hydraulics of overland flow on hillslopes: Dynamic and descriptive studies of hillslopes, geological survey professional paper, A1-A67*. U.S. Government Publishing Office.

Everaert, W. (1991). Empirical relations for the sediment transport capacity of interrill flow. *Earth Surface Processes and Landforms*, *16*(513–532), 1991.

Ferro, V. (1997). Applying hypothesis of self-similarity for flow-resistance law of small-diameter plastic pipes. *Journal of Irrigation and Drainage Engineering, ASCE*, *123*, 175–179.

Ferro, V. (1998). Evaluating overland flow sediment transport capacity. *Hydrological Processes*, *12*, 1895–1910.

Ferro, V. (1999). Friction factor for gravel-bed channel with high boulder concentration. *Journal of Hydraulic Engineering, ASCE*, *125*, 771–778.

Ferro, V. (2017). New flow resistance law for steep mountain streams based on velocity profile. *Journal of Irrigation and Drainage Engineering, ASCE*, *143*(04017024), 1–6.

Ferro, V. (2018a). Flow resistance law under equilibrium bed-load transport conditions. *Flow Measurement and Instrumentation*, *64*, 1–8. https://doi.org/10.1016/j.flowmeasinst.2018.10.008

Ferro, V. (2018b). Assessing flow resistance in gravel bed channels by dimensional analysis and self-similarity. *Catena*, *169*, 119–127. https://doi.org/10.1016/j.catena.2018.05.034

Ferro, V., & Pecoraro, R. (2000). Incomplete self-similarity and flow velocity in gravel bed channels. *Water Resources Research*, *36*, 2761–2770.

Ferro, V., & Porto, P. (2018a). Applying hypothesis of self-similarity for flow resistance law in Calabrian gravel-bed rivers. *Journal of Hydraulic Engineering, ASCE*, *140*(04017061), 1–11. https://doi.org/10.1061/(ASCE)HY.1943-7900.0001385

Ferro, V., & Porto, P. (2018b). Assessing theoretical flow velocity profile and resistance in gravel bed rivers by field measurements. *Journal of Agricultural Engineering*, *XLIX*, 220–227. https://doi.org/10.4081/jae.2018.810

Foster, G. R., Flanagan, D. C., Nearing, M. A., Lane, L. J., Risse, L. M., & Finkner, S. C. (1995). Hillslope erosion component. In D. C. Flanagan & M. A. Nearing (Eds.), NSERL Report No. 10 *USDA water erosion prediction project Hillslope profile and watershed model documentation* (p. 12). USDA-ARS National Soil Erosion Research Laboratory.

Govers, G.. (1990). Empirical relationships on the transporting capacity of overland flow, transport and deposition processes. *Proceedings of the Jerusalem Workshop*, March–April 1987, IAHS, *189*, 45–63.

Govers, G., Gimenez, R., & Van Oost, K. (2007). Rill erosion: Exploring the relationship between experiments, modeling and field observations. *Earth Science Reviews*, *8*, 87–102.

Hessel, R., Jetten, V., & Guanghui, Z. (2003). Estimating Manning's n for steep slopes. *Catena*, *54*, 77–91.

Jiang, F., Gao, P., Si, X., Zhan, Z., Zhang, H., Lin, J., Ji, X., Wang, M. K., & Huang, Y. (2018). Modelling the sediment transport capacity of flows in nonerodible rills. *Hydrological Processes*, *32*, 3852–3865.

Kowobari, T. S., Rice, C. E., & Garton, J. E. (1972). Effect of roughness elements on hydraulic resistance for overland flow. *Transaction of the ASAE*, *15*, 979–984.

Nearing, M. A., Foster, G. R., Lane, L. J., & Finkner, S. C. (1989). A process-based soil erosion model for USDA-water erosion prediction project technology. *Transactions of the ASAE*, *32*, 1587–1593.

Nearing, M. A., Polyakov, V. O., Nichols, M. H., Hernandez, M., Li, L., Zhao, Y., & Armendariz, G. (2017). Slope–velocity equilibrium and evolution of surface roughness on a stony hillslope. *Hydrology and Earth System Sciences*, *21*, 3221–3229.

Nicosia, A., Di Stefano, C., Palmeri, V., Pampalone, V., & Ferro, V. (2020a). Flow resistance of overland flow on a smooth bed under simulated rainfall. *Catena*, *187*, 104351. https://doi.org/10.1016/j.catena.2019.104351

Nicosia, A., Di Stefano, C., Palmeri, V., Pampalone, V., Ferro, V., & Nearing, M. A. (2019). Testing a new rill flow resistance approach using the water erosion prediction project experimental database. *Hydrological Processes*, *33*, 616–626.

Nicosia, A., Di Stefano, C., Pampalone, V., Palmeri, V., Ferro, V., & Nearing, M. A. (2020b). Testing a theoretical resistance law for overland flow on a stony hillslope. *Hydrological Processes*, *34*, 2048–2056.

Nicosia, A., Di Stefano, C., Pampalone, V., Palmeri, V., Ferro, V., Polyakov, V., & Nearing, M. A. (2020c). Testing a theoretical resistance law for overland flow under simulated rainfall with

different types of vegetation. *Catena*, *189*, 104482. https://doi.org/10.1016/j.catena.2020.104482

Peng, W., Zhang, Z., & Zhang, K. (2015). Hydrodynamic characteristics of rill flow on steep slopes. *Hydrological Processes*, *29*, 3677–3686.

Poesen, J. (2018). Soil erosion in the Anthropocene: Research needs. *Earth Surface Processes and Landforms*, *43*, 64–84. https://doi.org/10.1002/esp.4250

Polyakov, V., Stone, J., Holifield Collins, C., Nearing, M. A., Paige, G., Buono, J., & Gomez-Pond, R. (2018). Rainfall simulation experiments in the southwestern USA using the walnut gulch rainfall simulator. *Earth System Science Data*, *10*, 19–26. https://doi.org/10.5194/essd-10-19-2018

Powell, D. M. (2014). Flow resistance in gravel-bed rivers: Progress in research. *Earth-Science Reviews*, *136*, 301–338.

Prosser, I., & Rustomji, P. (2000). Sediment transport capacity relations for overland flow. *Progress in Physical Geography*, *24*, 179–193.

Sajjadi, S. A., & Mahmoodabadi, M. (2015). Sediment concentration and hydraulic characteristics of rain-induced overland flows in arid land soils. *Journal of Soils and Sediments*, *15*, 710–721.

Smith, M. W., Cox, N. J., & Bracken, L. J. (2007). Applying flow resistance equations to overland flows. *Progress in Physical Geography*, *31*(4), 363–387. https://doi.org/10.1177/0309133307081289

Takken, I., & Govers, G. (2000). Hydraulics of interrill overland flow on rough, bare soil surfaces. *Earth Surface Processes and Landforms*, *25*, 1387–1402.

Toy, T. J., Foster, G. R., & Renard, K. G. (2002). *Soil erosion: Processes, prediction, measurement, and control*. John Wiley & Sons.

Wu, B., Wang, Z. L., Shen, N., & Wang, S. (2016). Modelling sediment transport capacity of rill flow for loess sediments on steep slopes. *Catena*, *147*, 453–462.

Xiao, H., Liu, G., Liu, P., Zheng, F., Zhang, J., & Hu, F. (2017a). Response of soil detachment rate to the hydraulic parameters of concentrated flow on steep loessial slopes on the loess plateau of China. *Hydrological Processes*, *31*, 2613–2621.

Xiao, H., Liu, G., Liu, P., Zheng, F., Zhang, J., & Hu, F. (2017b). Sediment transport capacity of concentrated flows on steep loessial slope with erodible beds. *Scientific Reports*, *7*, 2350. https://doi.org/10.1038/s41598-017-02565-8

Yoon, Y. N., & Wenzel, H. G. (1971). Mechanics of sheet flow under simulated rainfall. *Journal of Hydraulic Division ASCE*, *97*, 1367–1386.

Zhang, G., Liu, B., Han, Y., & Zhang, X. C. (2009). Sediment transport and soil detachment on steep slopes: I. Transport capacity estimation. *Soil Science Society of America Journal*, *73*, 1291–1297.

Zhang, G., Wang, L., Tang, K., Luo, R., & Zhang, X. C. (2011). Effects of sediment size on transport capacity of overland flow on steep slopes. *Hydrological Sciences Journal*, *56*(7), 1289–1299. https://doi.org/10.1080/02626667.2011.609172

How to cite this article: Nicosia, A., Guida, G., Di Stefano, C., Pampalone, V., & Ferro, V. (2022). Slope threshold for overland flow resistance on sandy soils. *European Journal of Soil Science*, *73*(1), e13182. https://doi.org/10.1111/ejss.13182